PROCEEDINGS OF SCIENCE

Application of Photon Strength Functions to (n,γ) measurements with the n_TOF TAC

C. Guerrero[*1], **U. Abbondanno**[4], **G. Aerts**[6], **H. Álvarez-Pol**[12], **F. Alvarez-Velarde**[1], **S. Andriamonje**[6], **J. Andrzejewski**[19] , **P. Assimakopoulos** [8], **L. Audouin** [6], **G. Badurek**[9], **P. Baumann**[10], **F. Bečvář**[11], **E. Berthoumieux**[6], **S. Bisterzo**[5,1], **M. Calviani**[26], **F. Calviño**[13], **D. Cano-Ott**[1], **C. Carrapiço**[16], **R. Capote**[3,15], **P. Cennini**[17], **V. Chepel**[18], **E. Chiaveri**[17], **N. Colonna**[7], **G. Cortes**[13], **A. Couture**[20], **J. Cox**[20], **M. Dahlfors**[17], **S. David**[21], **I. Dillman**[14], **R. Dolfini**[22], **C. Domingo Pardo**[14] **W. Dridi**[1], **I. Duran**[12], **C. Eleftheriadis**[23], **L. Ferrant**[21], **A. Ferrari**[17], **R. Ferreira-Marques**[18], **H. Frais-Koelbl**[6], **K. Fujii**[4], **W. Furman**[24], **R. Gallino**[5], **I. Goncalves**[18], **E. Gonzalez-Romero**[1], **A. Goverdovski**[25], **F. Gramegna**[26], **E. Griesmayer**[6], **F. Gunsing**[6], **B. Haas**[27], **R. Haight**[28], **M. Heil**[14], **A. Herrera-Martinez**[17], **M. Igashira**[29], **S. Isaev**[21], **E. Jericha**[9], **Y. Kadi**[17], **F. Käppeler**[14], **D. Karamanis**[8], **D. Karadimos**[8], **M. Kerveno,**[10], **V. Ketlerov**[25,17], **P. Koehler**[30], **V. Konovalov**[24,17], **E. Kossionides**[31], **M. Krtička**[11], **C. Lamboudis**[8], **H. Leeb**[9], **A. Lindote**[18], **I. Lopes**[18], **M. Lozano**[15], **S. Lukic**[10], **J. Marganiec**[19], **S. Marrone**[7], **T. Martínez**[1], **C. Massimi**[39], **P. Mastinu**[26], **A. Mengoni**[3,17], **P.M. Milazzo**[4], **C. Moreau**[4], **M. Mosconi**[14], **F. Neves**[18], **H. Oberhummer**[9], **M. Oshima**[32], **S. O'Brien**[20], **J. Pancin**[6], **C. Papachristodoulou**[8], **C. Papadopoulos**[33], **C. Paradela**[12], **N. Patronis**[8], **A. Pavlik**[34], **P. Pavlopoulos**[35], **L. Perrot**[6], **R. Plag**[14], **A. Plompen**[36], **A. Plukis**[6], **A. Poch**[13], **C. Pretel**[13], **J. Quesada**[15], **T. Rauscher**[37], **R. Reifarth**[28], **M. Rosetti**[38], **C. Rubbia**[22], **G. Rudolf**[10], **P. Rullhusen**[36], **J. Salgado**[16], **L. Sarchiapone**[17], **I. Savvidis**[23], **C. Stephan**[21], **G. Tagliente**[7], **J.L. Tain**[40], **L. Tassan-Got**[21], **L. Tavora**[16], **R. Terlizzi**[7], **G. Vannini**[39], **P. Vaz**[16], **A. Ventura**[38], **D. Villamarin**[6], **M. C. Vincente**[6], **V. Vlachoudis**[17], **R. Vlastou**[33], **F. Voss**[14], **S. Walter**[14], **H. Wendler**[17], **M. Wiescher**[20], **K. Wisshak**[14]

The n_TOF Collaboration

[1]*Centro de Investigaciones Energeticas Medioambientales y Technologicas, Madrid, Spain;* [3]*International Atomic Energy Agency, NAPC-Nuclear Data Section, Vienna, Austria;* [4]*Istituto Nazionale di Fisica Nucleare, Trieste, Italy;* [5]*Dipartimento di Fisica Generale, Università di Torino, Italy;* [6]*CEA/Saclay - DSM, Gif-sur-Yvette, France;* [7]*Istituto Nazionale di Fisica Nucleare, Bari, Italy;* [8]*University of Ioannina, Greece;* [9]*Atominstitut der Österreichischen Universitäten,Technische Universität Wien, Austria;* [10]*Centre National de la Recherche Scientifique/IN2P3 - IReS, Strasbourg, France;* [11]*Charles University, Prague, Czech Republic;* [12]*Universidade de Santiago de Compostela, Spain;* [13]*Universitat Politecnica de Catalunya, Barcelona, Spain;* [14]*Forschungszentrum Karlsruhe GmbH (FZK), Institut für Kernphysik, Germany;* [15]*Universidad de Sevilla, Spain;* [16]*Instituto Tecnológico e Nuclear(ITN), Lisbon, Portugal;* [17]*CERN, Geneva, Switzerland;* [18]*LIP - Coimbra & Departamento de Fisica da Universidade de Coimbra, Portugal;* [19]*University of Lodz, Lodz, Poland;* [20]*University of Notre Dame, Notre Dame, USA;* [21]*Centre National de la Recherche Scientifique/IN2P3 - IPN, Orsay, France;* [22]*Università degli Studi Pavia, Pavia, Italy;* [23]*Aristotle University of Thessaloniki, Greece;* [24]*Joint Institute for Nuclear Research, Frank Laboratory of Neutron Physics, Dubna, Russia;* [25]*Institute of Physics and Power Engineering, Kaluga region, Obninsk, Russia;* [26]*Istituto Nazionale di Fisica Nucleare(INFN), Laboratori Nazionali di Legnaro, Italy;* [27]*Centre National de la Recherche Scientifique/IN2P3 - CENBG, Bordeaux, France;* [28]*Los Alamos National Laboratory, New Mexico, USA;* [29]*Tokyo Institute of Technology, Tokyo, Japan;* [30]*Oak Ridge National Laboratory, Physics Division, Oak Ridge, USA;* [31]*NCSR, Athens, Greece;* [32]*Japan Atomic Energy Research Institute, Tokai-mura, Japan;* [33]*National Technical University of Athens, Greece;* [34]*Institut für Isotopenforschung und Kernphysik, Universität Wien, Austria;* [35]*Pôle Universitaire Léonard de Vinci, Paris La Défense, France;* [36]*CEC-JRC-IRMM, Geel, Belgium;* [37]*Department of Physics and Astronomy - University of Basel, Basel, Switzerland;* [38]*ENEA, Bologna, Italy;* [39]*Dipartimento di Fisica, Università di Bologna, and Sezione INFN di Bologna, Italy;* [40]*Instituto de Física Corpuscular, CSIC-Universidad de Valencia, Spain*
E-mail: carlos.guerrero@ciemat.es

PoS(PSF07)006

PROCEEDINGS OF SCIENCE

The neutron capture cross section measurements at the CERN n_TOF facility are performed using a new detection system, the segmented Total Absorption Calorimeter (TAC). All measurements are performed in reference to the well known ^{197}Au σ(n,γ).

The accuracy of the measurements depends on the accuracy of the TAC detection efficiency, which is calculated by means of Monte Carlo simulations. In this MC simulation photon strength functions and level densities play a major role as ingredients used for the generation of primary events, that is the electromagnetic cascades following the (n,γ) process. We have calculated the TAC detection efficiency for the case of ^{197}Au(n,γ) by adjusting the photon strength functions of ^{198}Au so that the simulation reproduces the experimental data. Both the MC method and the uncertainty of the results are discussed.

Workshop on Photon Strength Functions and Related Topics
June 17-20, 2007
Prague, Czech Republic

*Speaker.

1. Introduction

The n_TOF Total Absorption Calorimeter (TAC) [1] is a segmented assembly of 40 BaF_2 crystals used for neutron capture measurements [2] at the CERN n_TOF facility [3]. It is the ideal device for measurements of low mass radioactive samples because of its segmentation and high total absorption efficiency. These two characteristics can be used to discriminate the different background components from the capture events attending to the energy deposited in the TAC (E_{sum}) and the number of crystals fired in each event, so-called crystal multiplicity (m_γ). The conditions $2.5<E_{sum}<7.5$ MeV and $m_\gamma>2$ are such that the capture to background ratio is maximized and are referred herafter as *analysis conditions*.

The accurate calculation of the detection efficiency (ε_{TAC}) of the detection device is crucial in the determination of the capture cross section. This ε_{TAC} is nearly 100% due to the characteristics of the device: $\sim 4\pi$ solid angle coverage with 15 cm thick BaF_2 crystals. However, when the *analysis conditions* are applied the number of detected events decreases and ε_{TAC} needs to be calculated by MC simulations. The MC simulation of the TAC includes the generation of primary events and the tracking of the particles through the detector assembly.

The difficulties associated to the generation of (n,γ) primary events, that is the electromagnetic cascades following any capture reaction, are related to the large number of nuclear levels in the region of intersest, that is below the neutron separation energy S_n. In this energy range, statistical models are needed to complement the experimental information on the nuclear levels scheme and the transitions probabilities between levels. Moreover, the parameters of the different statistical models are usually adjusted from experimental information and their validity is restricted to the energy range under study.

In the case of photon strength functions (PSF) used for the calculation of the transition probabilities, the available parameterizations are mostly intended to reproduce photoabsorption measurements with transitions of 5 MeV and above. Therefore a new parameterization may be needed to study the lower energy transitions that appear in (n,γ) reactions.

In this work, the detection efficiency of the TAC with and without analysis conditions is calculated for the case of ^{197}Au(n,γ), which is the reference for many n_TOF measurements. The generalities of the MC code and the primary event generator are described in sections 2 and 3. The adjustment of the PSF for ^{197}Au(n,γ) reactions and the results of the MC simulations are discussed in section 4. Finally, the uncertainty of the results is calculated in section 5.

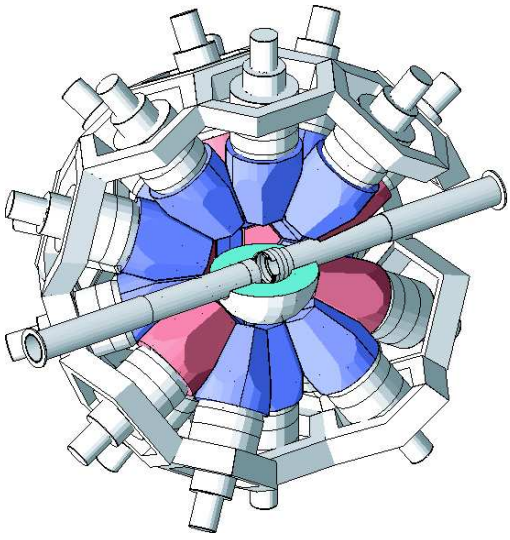

Figure 1: *View of the Total Absorption Calorimeter as it is implemented in GEANT4.*

2. Monte Carlo simulation code

The MC code is based in the GEANT4[4] simulation tool with the Standard Electromagnetic package. The geometry of the detector assembly is implemented with high accuracy including details down to millimeter scale. This is shown in Fig.1 where half of the TAC is shown together with the neutron absorber, the beam line, the support structure, etc.

The photons and electrons emitted during the de-excitation of the nucleus after the neutron capture reaction are transported through the detector assembly and the interactions taking place in the BaF_2 crystals are tracked and recorded. The individual interactions are grouped into capture events with given m_γ and E_{sum} by performing a coincidence analysis capable of taking into account experimental effects such as signal summing, dead-time losses, detection threshold, energy resolution, etc.

The TAC geometry, particle tracking and coincidence analysis software have been successfully validated by comparison of the simulations with the measurements of well known γ-ray calibration sources [5].

3. Neutron Capture Event Generator

Many experiments in nuclear physics need physics event generators which are used to drive the simulations, prepare experimental proposals and test the analysis methods. In many cases, the validity of the results may depend upon the quality of the event generators and the MC simulations.

An *Event Generator* is a piece of code which generates a list of events, where each event contains a set of particles created simultaneously. Typically each particle is parameterized by its type, initial position and momentum vector.

The generation of capture cascades following neutron capture reactions requires the complete knowledge of the nuclear level scheme (energy, spin and parity of all levels below S_n) and transition probabilities between levels. This information is known experimentally only in a reduced energy range above the ground state and models are required to describe these quantities in the complete excitation energy range of interest.

The cascade generator used in this work has been already used for previous n_TOF measurement with total energy detectors, see for example [6]. In this event generator the nuclear level scheme is divided in two ranges, as shown in Fig. 2:

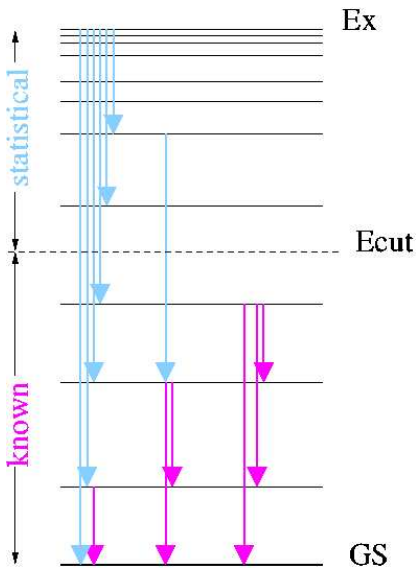

Figure 2: *Nuclear level scheme used in the capture cascade generator model.*

- The lower energy range corresponds to experimentally known levels (energy, spin and parity) with known transitions probabilities. This information is retrieved from the Evaluated

Nuclear Structure Data Files [7] and allows the exact calculation of the low energy part of the branching ratio matrix. The electron conversion process is included in this energy range from the binding energies of the K-,L- and M-shells, fluorescence yields and internal conversion coefficients.

- Between the cut-off energy E_{cut} and the neutron capture level at $E_{cap} \simeq S_n + E_n$, the levels and transitions are calculated by means of models. In these models, individual levels are created by sampling the level density distribution given by the Back Shifted Fermi Gas (BSFG) model, and the transition probabilities between the generated levels are calculated for E1, M1 and E2 transitions from the modeled PSF.

Starting at the capture level, with known spin and parity, a random sampling is performed in order to generate a number of cascades sequentially, each generated as follows:

1. The branching ratio matrix for E1, M1 and E2 transitions is calculated from the capture level to all underlying levels; which can be known or generated using the BSFG model.
2. The transition to a new level is sorted randomly according to the branching ratio matrix.
3. If the new level is in the statistical energy range, the branching ratio matrix for the new level is calculated for all underlying levels. Otherwise, the branching ratio matrix is known from ENSDF and does not need to be calculated.
4. Repeat step 2 until the ground (or metastable) state is reached.

The available parameterizations of the models describing PSF are usually the result of the study of photoabsorption experiments. In these experiments the PSF can be studied for transitions of high energy, usually above the S_n. For this reason the available PSF are only a good starting point to study low energy transitions, as it is the case in this work, but they may need to be adjusted to reproduce the experimental data.

4. Results for ^{197}Au(n,γ)

The nuclear level scheme of ^{198}Au is known experimentally up to $\sim$1.4 MeV [7], above this energy the nucleus is described by statistical models as previously discussed. In this work, the BSFG model parameters recommended in the RIPL-2 [8] data base have been chosen for the description of the level density and the parameterization of Kopecky et al. [9] for the calculation of E1, M1 and E2 PSF, referred herafter as *initial PSF* (see Tab. 1). In the *initial PSF*, the energy dependence of the E1 transition probability is assumed to follow the shape of a Generalized Lorentzian as described in [9], while the standard Lorentzian shape is assumed for the description of M1 and E2 transition probabilities.

Fig. 3 shows the comparison between the experimental data (black) and the simulation using the *initial PSF* (blue) of E_{sum} and m_γ for the case of ^{197}Au(n,γ) at the top of the 4.9 eV resonance. The differences that can be observed between these distributions are expected and are due to the inaccuracy of the PSF in the energy range under study in this work. A good reproduction of the experimental data can be only obtained after the implementation of a new parameterization of the

Table 1: *Initial PSF for ^{198}Au (Kopecky et al.[9])*

	E1		M1	E2
E (MeV)	13.72	5.8	7.05	10.81
Γ (MeV)	4.61	1.5	4.00	3.73
σ_0 (mb)	541.0	6.0	1.12	5.03

PSF. It is important to remark that the aim of the adjustment of the PSF is not to obtain a shape for the PSF valid for all transition energies but a PSF parameterization that implemented in the simulation code gives compatible results with the experimental data.

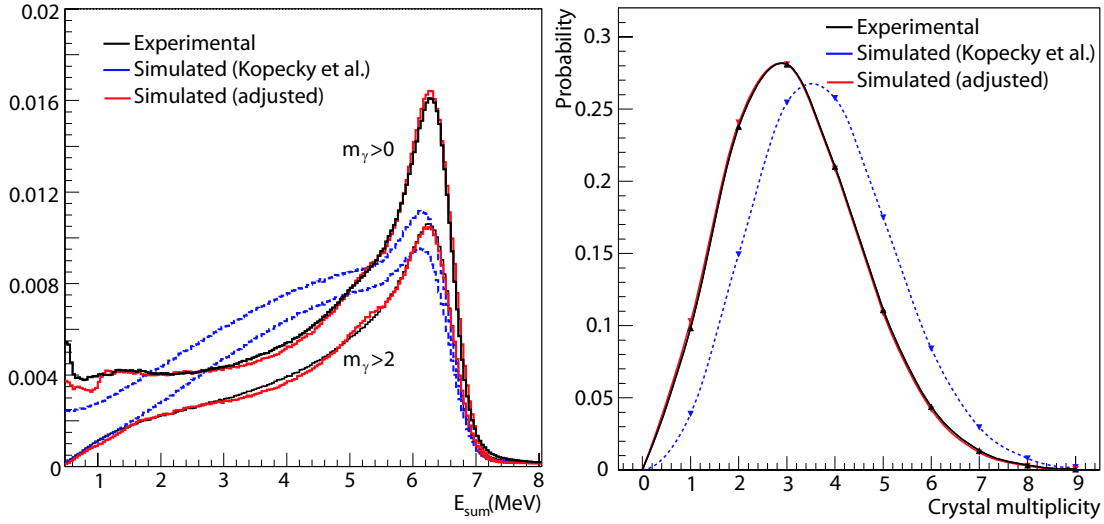

Figure 3: *TAC response to ^{197}(n,γ): deposited energy (left) and crystal multiplicity (right). Black: Experimental. Blue: Simulated using the initial PSF. Red: Simulated using the adjusted PSF.*

A systematic study of the TAC response to variations in the PSF parameters shows that the simulated and experimental data become compatible when the following changes are applied:

- increase the intensity of E1 transitions around S_n in order to decrease m_γ, because these are the only possible transitions from the capture state (2+) to directly populate the lowest laying levels, 0, 55 and 192 keV with spin and parity 2-,1- and 1-, respectively.
- introduce two small resonances (Kopecky et al. introduce only one) for E1 transitions at 1.1 and 5.5 MeV,
- decrease the energy and width of the Lorentzian shape describing M1 transitions.

Applying these changes to the *initial PSF* it is possible t find several parameterizations that allow the reproduction of the experimental data with high accuracy. An example is given in Tab. 2 and the associated TAC response is shown as a red line in Fig. 3, Fig. 4 and Fig. 5. The average m_γ of the simulation (3.38) differs less than 1% from the experimental value (3.40) and the E_{sum} spectrum is reproduced even when the analysis condition of m_γ>2 is applied.

Table 2: *Parameters of the ^{198}Au PSF adjusted below S_n to reproduce the n_TOF data.*

	E1			M1	E2
E (MeV)	6.38	5.5	1.1	5.05	10.81
Γ (MeV)	0.042	1.5	0.8	1.5	3.73
σ_0 (mb)	500.	6.5	0.2	2.0	5.03

The deposited energy in each crystal ($E_{crystal}$) for events with a given m_γ is more sensitive to the de-excitation pattern of the compound nucleus than the m_γ and E_{sum} distributions. This is shown in Fig. 4, where only events $E_{sum} > 2$ MeV are selected. In this case, the simulation with the *adjusted PSF* (red line), again, reproduces very accurately the experimental data (black line) for all m_γ.

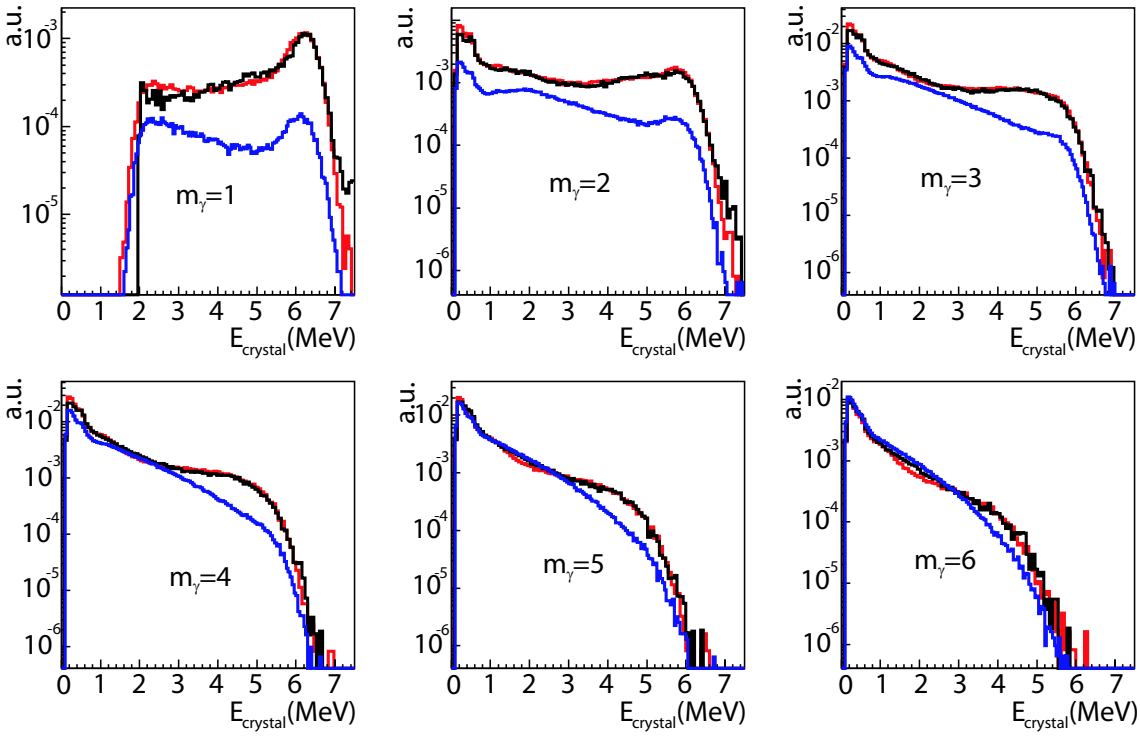

Figure 4: *$E_{crystal}$ for ^{197}Au(n,γ) events with E_{sum} >2 MeV for each m_γ. Black: measured. Blue: simulated with initial PSF. Red: simulated with adjusted PSF.*

5. Uncertainty in the detection efficiency

As stated below, there is more than one parameterization that can be used to reproduce the experimental data with better or worse accuracy. In order to estimate the uncertainty in ε_{TAC} associated to the arbitrariness in the choice of the PSF parameters, the TAC response has been simulated (colored-dashed lines in Fig. 5) for several PSF that reproduce more or less the experimental data (black-solid line in Fig. 5). The red dashed-line correspond to PSF_3, which is the one discussed in

the previous section (see Tab. 2) and gives the best results. The detection efficiency is calculated for the simulations with the different PSF used in Fig. 5 and the results summarized in Tab.3. In the table, the value of ε_{TAC} is shown for the case of no conditions in E_{sum} and m_γ and for the case of the analysis conditions ($2.5<E_{sum}(MeV)<7.5$ and $m_\gamma>2$).

Table 3: Uncertainty in ε_{TAC} due to the election of the appropriate PSF.

	PSF_1	PSF_2	PSF_3	PSF_4	PSF_5	RMS
ε_{eff}	0.932	0.929	0.932	0.925	0.925	**0.003**
ε_{eff} (m_γ & E_{sum})	0.563	0.540	0.533	0.511	0.495	**0.023**

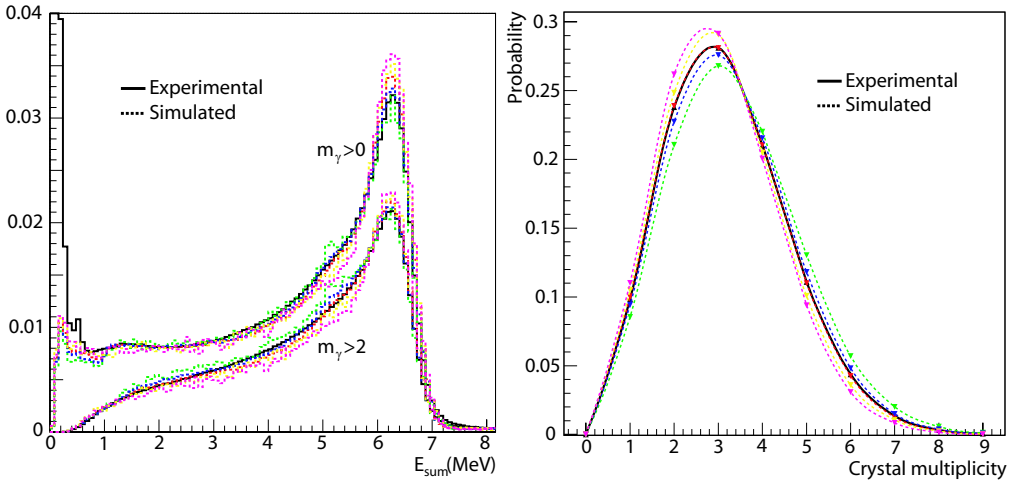

Figure 5: *Deposited energy (left) and crystal multiplicity (right) distributions. Black: experimental. Colored: Simulation using different photon strength functions (PSF_{1-5}).*

From the values in Tab. 3, the final values of ε_{TAC} and their uncertainty with and without analysis conditions can be estimated as:

$$\varepsilon_{TAC} = 0.932 \pm 0.003 \tag{5.1}$$

$$\varepsilon_{TAC}^{analysis\ conditions} = 0.533 \pm 0.023 \tag{5.2}$$

6. Conclusions

A method for calculating the TAC detection efficiency for any condition in m_γ & E_{sum} has been developed and validated in this work. This is done by means of a Monte Carlo simulation of the complete process, that is the generation of capture events and the tracking of the generated particles trough the detector assembly. The generation of capture events is based on the nuclear level scheme and transition probabilities between levels. The necessary information is available in the form of experimental data at low excitation energies and statistical models at higher energies. In order to reproduce the experimental TAC response, in the form of deposited energy spectra

and crystal multiplicity distributions, it has been necessary to adjust the parameters describing the photon strength functions of E1, M1 and E2 transitions.

It has been shown that it is possible to reproduce the experimental TAC response for different conditions in m_γ and E_{sum} and to calculate the detection efficiency under the analysis conditions with an accuracy better than 4.5%.

It is important to underline the significant amount of information that the TAC measurements are able to provide regarding energy deposition and crystal multiplicity distributions for selected conditions. This information can be used to study photon strength functions in a wide energy range that is not easy to study by means of other experimental techniques. In particular, future plans include the systematic study of photon strength functions and the search of scissor resonance structures in the PSF of the Minor Actinides measured at n_TOF.

Acknowledgments

This work has been supported partially by the NTOF-ND-XADS project from the EU 5^{th} Framework Programme, the CIEMAT-ENRESA Agreement on the *"Separation and Transmutation of nuclear waste"* and the Spanish Plan Nacional de Física de Partículas under contract FPA2005-06918-C03-01.

References

[1] D. Cano-Ott et al., *Monte Carlo Simulation of the 4pi Total Absorption Calorimeter at n_TOF* n_TOF Internal Report (2003)

[2] C. Guerrero et al. (The n_TOF Collaboration) *The neutron capture cross sections of ^{237}Np(n,γ) and ^{240}Pu(n,γ) and its relevance in the transmutation of nuclear waste*,Proceedings of the Int. Conf on Nuclear Data for Sciences and Tech. ND2007, Nice-France (2007)

[3] The n_TOF Collaboration, *CERN n_TOF Facility: Performance Report*, CERN/INTC-O-011, INTC-2002-037 CERN-SL-2002-053 ECT (2006)

[4] S. Agostinelli et al. *Geant4 - A Simulation Toolkit*, Nucl. Inst. Meth. A **506** 250-303 (2003)

[5] C. Guerrero, *Simulación Monte Carlo del Calorímetro de Absorción Total de n_TOF*, Diploma Thesis, Universidad Complutense de Madrid, Spain (2005)

[6] C. Domingo-Pardo et al. (The n_TOF Collaboration) *New measurement of neutron capture resonances in ^{209}Bi*, Phys. Rev. C **74**, 025807 (2006)

[7] *Evaluated Nuclear Structure Data Files* http://www.nndc.bnl.gov/ensdf/

[8] *Handbook for calculations of nuclear reaction data, RIPL-2*.

[9] J.Kopecky and M. Uhl, *Test of γ-ray strength function in nuclear reaction model calculations*, Phys. Rev **41** 1941-1955 (1990)